B. D. Washo

Rheology and Modeling of the Spin Coating Process

Abstract: This study examines the spin coating process both experimentally and from a fundamental point of view. The analysis has produced a model and a quantitative relationship between spin coating thickness and pertinent material and process variables. The model predicts that the simplest and most reproducible results occur in a region which is independent of thickness and time and is characterized by low steady state radial flow on the substrate. The model also includes a time-dependent term, shown to be important for the region of high radial flow—fluids of relatively low viscosity and process conditions of relatively high speed and/or long times. Experimentally, Newtonian-like polyamide in iso-amyl alcohol solutions was examined on large rotating substrates, and measurements showed excellent correlation with the model. The sensitivity of the spin coating process to substrate size and shape is also reported and a comparison with other data in the literature, particularly on photoresist solutions, is presented. The potential applicability of the model to non-ideal fluids is also developed.

Introduction

The spin coating process has been used extensively, particularly in the electronics industry, and is a popular conformal technique for coating a planar substrate. Accordingly, applications of this process have ranged from photoresist and polyimide coatings on semiconductor silicon wafers to oxide coatings on memory disk-file substrates. Because of its wide usage, there exist extensive data on the process and many process parameter correlations.

Unfortunately, many of these correlations suffer several deficiencies: They tend to be inconsistent with the use of process and material variables, incomplete with regard to specification of process conditions, and not readily applicable to other applications; almost all such data are empirically, or at best semi-empirically, treated [1–4]. The questions of what causes a coating solution to behave in a predictable manner, and which process parameters or groupings of process parameters primarily govern the spin coating process, and with what priorities, are best developed through a fundamental approach and analysis.

The general problem of the flow of liquids on rotating substrates, including the coating process governed by this phenomenon, has received little attention in the literature. It appears that the spin coating process—approached from a fundamental point of view—should be useful toward understanding the nature of the process and produce constructive correlation between process and material parameters, thus improving process reproducibility and reliability.

The spin coating process studied in this report was used to provide protective overcoats for large lithographic glass substrates (sizes to 25 cm × 30 cm). The overcoat material was Milvex 4000 nylon (a modified dimerized di-acid-based polyamide resin, product of the General Mills Corporation). The Milvex material is known to have the following basic properties: It is transparent and inert with respect to uv radiation, has no optical impairment in photolithographic resolution, is wear and abrasion resistant, has a hydrophobic and anti-sticking surface, and enhances mask-usage longevity.

Since reference data provided no information with regard to the sensitivity of the spin coating process to substrate size and configuration, spin coatings on large masks were investigated experimentally as a function of substrate size and process and material variables. A theoretical model was also constructed to estimate these effects on the process.

The Milvex resin was used in solution with iso-amyl alcohol. Viscometry measurements on these solutions, containing solids in the range 0 to 15 weight percent, showed the solutions to be Newtonian-like over a shear-rate-ratio range of two decades; i.e., the viscosity was independent of shear rate (Fig. 1).

Historical review

Although there has been much research on the fluid-mechanical properties of falling liquid films (5), only in the last decade or so has attention been given to the flow of liquids on rotating substrates. Many of these studies have been directed toward heat transfer applications, such as in connection with turbine rotors, packed absorption towers, cooling towers, distillation columns, etc. [5–8].

The first reported applications of the spin process as a coating technique were for preparations of thin, uniform films of paint and varnish [9] and of asphalt [10]. One early study by Emslie et al. [11] used the spin coating process to apply conformal films of phosphor-photoresist to curvilinear surfaces of television faceplates. Emslie developed theoretical solutions for the change with time of the film thickness distribution of a Newtonian fluid on an infinite rotating plane, given initial values. In attempting to use his approach in our work, however, we were unable to reconcile the use of certain assumptions in his derivation and, in fact, our data appear to be contradictory. Acrivos et al. [12] followed Emslie's approach as applied to non-Newtonian liquids on a rotating disk and, interestingly, concluded that coating uniformity was virtually impossible for non-Newtonian fluids.

Epsig and Hoyle [13] investigated the phenomenon of wave formation in thin liquids on a rotating substrate and correlated their measurements with a modified, early theory of Nusselt [14]. Their work, basically in agreement with the conclusions of earlier falling film investigations [15–18], indicated that in order for waves to form, surface forces are important and the Reynolds number must be greater than four (a conservative minimum), where

$$Re = 4Q/\pi D\nu \qquad (1)$$

and Q, D, and ν are the volumetric flow rate, diameter, and kinematic viscosity, respectively. (It will be shown that wave formation is not important and need not be considered for the system studied in this report.)

Numerical solutions have been obtained by Dorfman [7] for initial film formation, and analytic solutions have been obtained for asymptotic or steady state behavior of the film by Aroesty [19] and by Gazley and Charwat [8]. These particular solutions were derived for Newtonian fluids, assuming in addition a constant liquid source at the center of the disk. (No time dependence of the solutions was addressed.)

In general, these early studies do not seem to be readily applicable to the spin coating problem. However, their results can be used to outline the general regions in which certain simplifying assumptions can be made in the spin coating case.

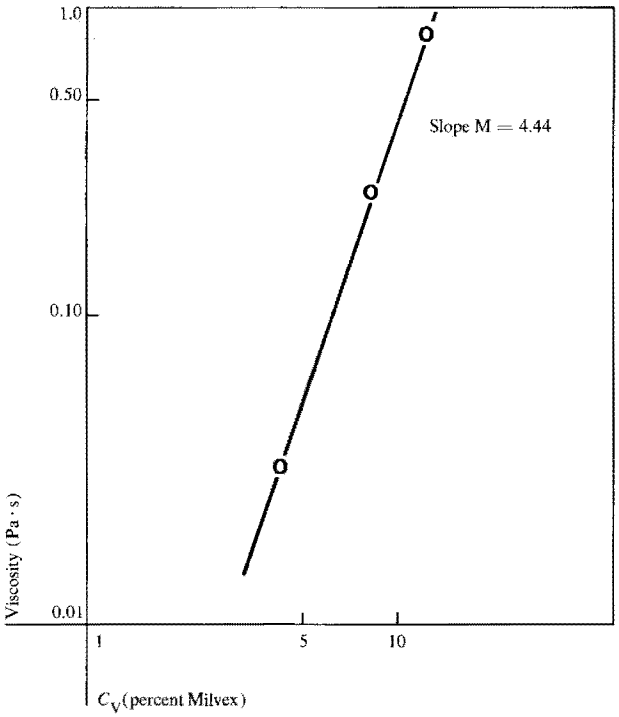

Figure 1 Newtonian viscosity of a Milvex 4000-iso-amyl alcohol mixture over a shear-rate-ratio range of 200:1.

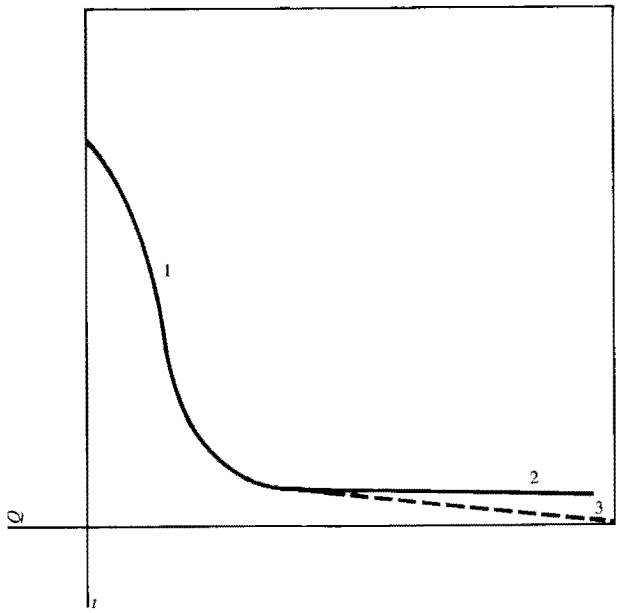

Figure 2 Volumetric flow of fluid in the radial direction, Q vs time t for the three flow regions: 1) predeveloping, 2) steady state, and 3) quasi-steady state.

Rheology of the spin coating process

The spin coating process can best be understood by considering the rheology or flow behavior of fluids on a rotating disk substrate.

Initially, the volumetric flow of liquid in the radial direction on the substrate is assumed to vary with time as indicated in Fig. 2. At $t = 0$, initial flooding and complete wetting of the surface substrate are assumed. (Surface tension phenomena are thus minimized, i.e., no waves, no dry spots, etc.) The disk is then accelerated to a specific rotational velocity, causing the bulk of the liquid to be sloughed off the disk. A steady state flow

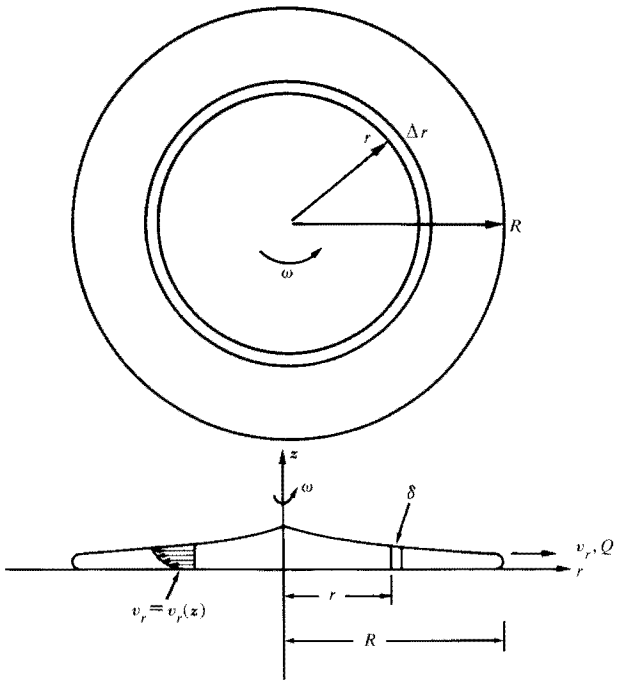

Figure 3 Flow rate Q and velocity profile $v_r(z)$ for a homogeneous fluid in flow developed on a spinning disk.

regime (region 2), which follows this predeveloping flow (region 1), is achieved in a relatively short time, and is characterized by $dQ/dt = 0$—a plateau region of relatively low and constant volumetric flow on, and of course off, the disk. This steady state regime also means that the average film thickness on the disk essentially does not change with time. If $dQ/dt \neq 0$, the average film thickness becomes time dependent (region 3) and is treated later as a separate case.

At this point, the spin coating process can be visualized by referring to Fig. 3, which shows the symmetrical flow pattern of a homogeneous liquid on a rotating disk. A fluid element in the form of an annulus moves symmetrically outward from the center of the disk to the perimeter, where the liquid is eventually lost if the process is continued long enough. At steady state, the fluid element experiences essentially two forces in balance on it: the outward centrifugal force of rotation (as opposed to the inward centripetal force of rotation) and the viscous shear force of the flowing annulus. Other forces such as body and Coriolis can be shown to be unimportant for the system studied in this report. The viscous flow of the annulus is reflected as a velocity profile in Fig. 3.

The steady state, constant temperature flow behavior is predicted to be a function of the fluid rheology—the particular material constitutive equation of the fluid—and the process parameters of rotational speed, disk size, and time. The flow profile is seen to be initially nonuniform with an apparent midpoint mound that is the source for the flow in the disk. Later in the process this flow is quickly damped to a more uniform profile. (The steady state profile, $\delta \approx r^{-\frac{2}{3}}$, where δ is the film thickness and r is the radial position, is shown later.) Furthermore, upon cessation of the spin coating process and subsequent drying or curing of the film on the substrate, surface tension forces aid in smoothing out the thickness profile to make it highly uniform and conformal. In this report all film thicknesses are given for the dry film.

• *Theoretical model*

Arbitrary flow behavior is completely generalized according to the equation of fluid motion in vector notation,

$$\rho\, D\mathbf{v}/Dt = \nabla \cdot \tau - \nabla \mathbf{P} + \rho \mathbf{g}, \tag{2}$$

where

$D\mathbf{v}/Dt$ = substantial time derivative of fluid velocity vector $\mathbf{v}$,
τ = stress tensor
$\nabla \mathbf{P}$ = pressure gradient vector,
$\rho \mathbf{g}$ = gravitational body force vector, and
ρ = density.

This equation is a phenomenological equation and must be coupled with a material constitutive equation in order to be completely solved. The simplest material is a fluid that obeys Newton's law of viscosity which, in one dimension, makes the fluid shear stress τ directly proportional to the shear rate; i.e., the viscosity is independent of the shear rate:

$$\tau = \mu\, \partial v/\partial z, \tag{3}$$

where μ is the viscosity (proportionality constant) and $\partial v/\partial z$ is the velocity gradient or shear rate in the z (coating thickness) direction. Coupling Newton's law of viscosity [Eq. (3) in a generalized form] with the equation of fluid motion, Eq. (2), one obtains the classical Navier-Stokes equation, which in vector form can be written as

$$\rho\, D\mathbf{v}/Dt = -\nabla \mathbf{P} + \nabla^2 \mathbf{v} + \rho \mathbf{g}. \tag{4}$$

This equation can be simplified and solved for the following conditions: steady state, constant pressure and temperature, rotationally symmetric flow of a homogeneous fluid on a spinning disk, net flow only in the radial direction, no evaporation loss (therefore μ = constant), and no body or surface forces (see Figs. 2 and 3 and the Appendix, Case A). Then, for any fluid in the general spin coating process, the following phenomenological (or state) equation can be shown to be a solution of Eq. (2):

$$\partial \tau_{rz}/\partial z = -\rho r \omega^2, \tag{5}$$

where τ_{rz} is the shear stress on the z face of a fluid ele-

ment arising from fluid momentum in the r direction, and z is the film thickness direction. This equation can be derived from another approach; see the Appendix, Case B. For a Newtonian fluid, the equivalent result that follows from the Navier-Stokes equation (or the combination of Eqs. (3) and (5) is

$$\partial \tau_{rz}/\partial z = \mu\, \partial^2 v_r/\partial z^2 = -\rho r\omega^2. \tag{6}$$

For the general non-Newtonian fluid, a more complicated material or fluid constitutive equation than (3) is required. Once ascertained, its combination with Eq. (5) allows, in principle, a solution of the problem. The simplest non-Newtonian fluid is the power-law fluid described in Eq. (7), with a constitutive equation analogous to the Newtonian model described in Eq. (3):

$$\tau = \mu\, dv/dz, \text{ where } \mu \equiv m|dv/dz|^{n-1}, \tag{7}$$

and m and n are model constants. Work and results on this power-law fluid model will be reported in a future paper.

Time-independent solution

By using the steady state assumption $dQ/dt = 0$, Eq. (6) can be shown to yield the following solution (see Appendix Case C):

$$\delta = KC_V(\nu/\omega^2R^2)^{\frac{1}{3}}, \tag{8}$$

where ν is the kinematic viscosity; C_V is the volume fraction of solids; ω is the angular velocity; R is the disk radius or average symmetrical dimension of the sample; δ is the dry coating thickness; Q is the volumetric flow rate; and K is a constant, $(81Q/16\pi)^{\frac{1}{3}}$.

Time-dependent solution

If $dQ/dt \neq 0$, then significant removal of liquid from the rotating disk occurs, seriously affecting the validity of Eq. (8). The steady state thickness has a time dependence as shown by region 3 of Fig. 2, where the plateau region at some arbitrary velocity now has a nonzero slope. This situation can occur for liquids of either relatively low viscosity or high rotational process speeds, and for long times. A quasi-steady state solution is similar to Eq. (8) but is modified by a time-dependent reduction factor (see Appendix, Case D):

$$\delta = KC_V\left(\frac{\nu}{\omega^2R^2}\right)^{\frac{1}{3}}\left[1 + 0.395K^2\left(\frac{\omega^2}{\nu R^4}\right)^{\frac{1}{3}} t\right]^{-\frac{1}{2}}. \tag{9}$$

Here t is the process time but it should be modified to $t - t'$, where t' is the initial time, assumed to be short (1 to 3 s), before flow develops on the disk.

Equation (9) reduces to Eq. (8) where there is no time dependence, or for high viscosity fluid films at low rotational speeds and for short times; these conditions are related and defined by the following simple test. To determine whether the spinning time over a range of conditions is an important parameter, and therefore requires the use of Eq. (9), one evaluates the ratio

$$t_{\text{process}}/t_{0.5}$$

which, in order to use Eq. (8), must be less than 0.01. This is the ratio of the actual process time to the time calculated as needed to reduce the coating thickness by a factor of two. The latter is obtained from

$$t_{0.5} = 7.60/(\omega^2/\nu)\delta_0^2, \tag{10}$$

where δ_0 is the desired coating thickness at $t \approx 0$ (see Appendix, Case D).

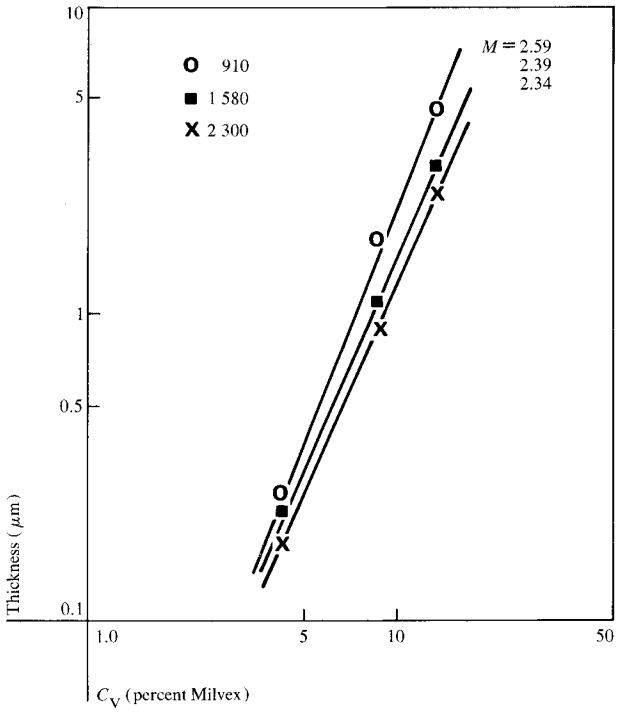

Figure 4 Spin coating thickness of a Milvex 4000-iso-amyl alcohol mixture on a 20.3-cm × 25.4-cm glass plate for three speeds of rotation; $M_{avg} = 2.44$, $M_{calc} = 2.47$.

Experimental results

Equation (8) can be tested by examining spin coating data on log-log graph paper, which allows determination of the characteristic exponents of the various parameters via slope measurements. Using the slope data of Fig. 1, which shows Newtonian viscosity correlated with Milvex-solid content on a volume basis ($\mu \approx C_V^{4.44}$), a calculation can be made to obtain a predicted value:

$$\nu^{\frac{1}{3}}C_V \approx \mu^{\frac{1}{3}}C_V \approx (C_V^{4.44})^{\frac{1}{3}}C_V = C_V^{2.47}. \tag{12}$$

The resulting exponent, 2.47, is in good agreement with the measured value of 2.44, which represents the average slope as shown in Fig. 4.

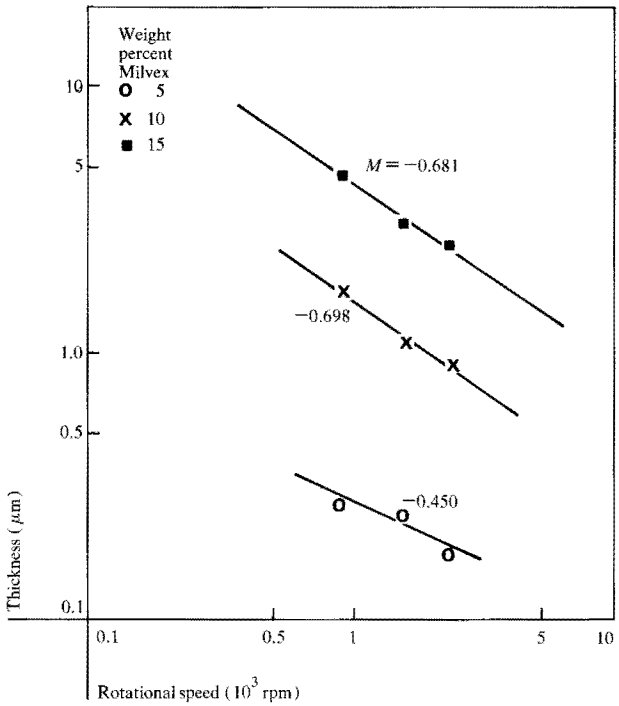

Figure 5 Spin coating thickness of a Milvex 4000-iso-amyl alcohol mixture on a 20.3-cm × 25.4-cm glass plate for three concentrations; $M_{calc} = -0.667$.

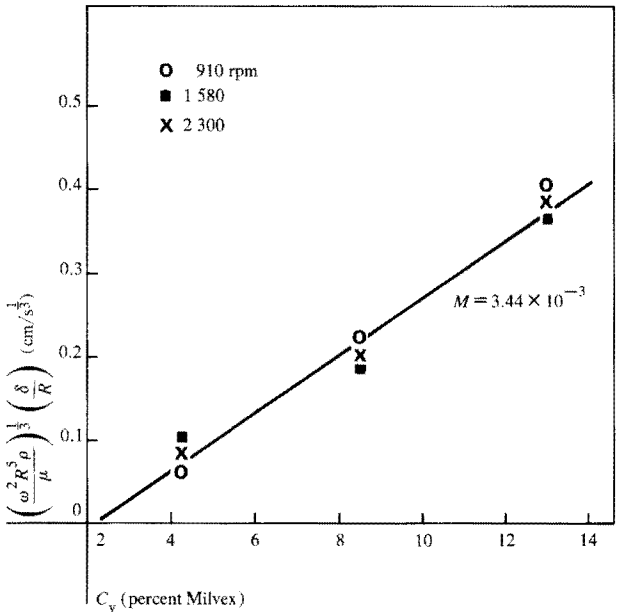

Figure 6 Reduced thickness parameter of a Milvex 4000-iso-amyl alcohol mixture for three rotational speeds.

The exponent on ω can be similarly tested (Fig. 5), and there is satisfactory agreement between the measured slope (−0.68) and the predicted value (−0.67). The case in which the slope was −0.45 is due to scatter in the data in the area of very thin film thickness.

All the data can be reduced and consolidated by plotting $(\omega^2 R^5 \rho/\mu)^{\frac{1}{3}}$ (δ/R) vs C_V (Fig. 6). The predicted linear fit of the data is shown with slope $M(Q)$, which allows determination of Q. This volumetric flow rate in the radial direction is found to be 2.53×10^{-8} cm^3/s, from $Q = 0.621M^3$. The model requires that Q be very small and relatively constant. In addition, experiments with coating times between 30 and 90 s show the coating thickness to be independent of time for the Milvex solutions. These data, together with Fig. 4 (small slope variation) show these assumptions to be essentially satisfied for this system.

The equation of the solid line in Fig. 6 is

$$(\omega^2 R^5 \rho/\mu)^{\frac{1}{3}} (\delta/R) = 3.44 \times 10^{-3} C_V - 7.50 \times 10^{-3},$$

$$\text{where } M(Q) = 3.44 \times 10^{-3}. \tag{12}$$

The assumption of neglecting wave fronts is validated by using the experimentally determined $Q = 2.53 \times 10^{-8}$ cm^3/s with Eq. (1) to demonstrate $Re \ll 1$. Coriolis effects are shown to be negligible (see Appendix, Case E).

The time-dependent reduction factor of Eq. (9) is shown not to be important for this system by calculating the ratio $t_{process}/t_{0.5}$. First, the lower bound of $t_{0.5}$ is calculated according to Eq. (10). For $\omega/2\pi = 2\,000$ rpm, $\mu = 30$ centipoise (cP), $\rho = 0.8$ g/cm^3, $\delta_0 = 1$ μm, and $t_{process} = 30$ s, we find

$$t_{process}/t_{0.5} = 0.0046, \tag{13}$$

which is well below 0.01; i.e., a 30-s process time does not affect the steady state plateau region even for worst-case conditions, and thus Eq. (8) is valid for this system.

The shape of the substrate was not found to be a significant factor influencing spin coating results or conformality of the coating (excluding the film edges and corners). For rectangular plates, the observed area of film uniformity (ten film thickness measurements were taken per quadrant and averaged) appeared to be that of an inscribed ellipse, which suggested an average symmetrical dimension to be

$$2R = D^* = [\tfrac{1}{2}(A^2 + B^2)]^{\frac{1}{2}}, \tag{14}$$

where A and B are the sides of the rectangle.

Data on spin coating thickness as a function of disk radius or, more generally, of the average symmetrical dimension D^*, were not found to follow the predicted $R^{-\frac{2}{3}}$ dependence. Figure 7 shows data on large and small rectangular mask plates and, in one case, on a silicon wafer. (See Table 1.) The dotted line indicates the theoretical curve expected for the smaller plates, referenced relative to Sample 4. These data show the actual coating

Table 1 "Average" dimension of substrates.

Sample	*A*(cm)	*B*(c)	*D**(cm)
1	6.35[a]		6.35
2	8.84[b]	8.84[b]	8.84
3	16.2	27.9	22.8
4	20.3	25.4	23.0
5	25.4	30.5	28.1

[a]Round substrate, silicon wafer.
[b]Chromium mask.

thickness to be less than predicted and, furthermore, to asymptotically become independent of plate size beyond $D^* = 18$ cm. The D^* or R of the model does correlate better with the general thickness gradient or profile across the sample surface of a *flowing* film during the spin coating process [8].

Comparison with other data

Though not specifically investigated, we expect the model to be applicable to photoresist polymer solutions, and correlation with such data in the literature was found, in general, to be good. For example, data from Schwartz [2] on computer-generated empirical equations for the spin coating of Eastman Kodak KTFR photoresist indicate a concentration-dependence exponent of 2.2 and an angular velocity-dependence exponent of −0.68, both in good agreement with the model. In a similar manner, the data of Kelley [20] on KTFR gave a value of −0.70.

The data of Zielinski [21] on DuPont RC5057 polyimide in *n*-methyl pyrrolidone show good correlation with the predicted slope of −0.667 for $\delta - \omega$ in Fig. (8). The data of Taylor [3] show $\delta - \omega$ slopes of −0.657, −0.602, and −0.430 for modified Eastman Kodak photoresist (KMER) solutions of viscosity 65, 85, and 110 cP (0.065, 0.085, and 0.11 Pa · s), respectively.

Summary

The spin coating model appears to accurately describe the spin coating process for material systems that behave in a Newtonian manner. This was found to be the case for the polymer solutions examined in this study. Furthermore, the model predicts that the simplest and most reproducible results of the spin coating process occur when the process is operated in a region characterized by low, steady state, radial flow. High radial flow involves a more complicated time-dependent behavior, which becomes important for low viscosity fluid films at relatively high process speeds or long times, but this is also described by the model. As a corollary of the treatment, a measure of the "Newtonian-ness" of a fluid is the agreement between the experimental data and the characteristic exponents of the model.

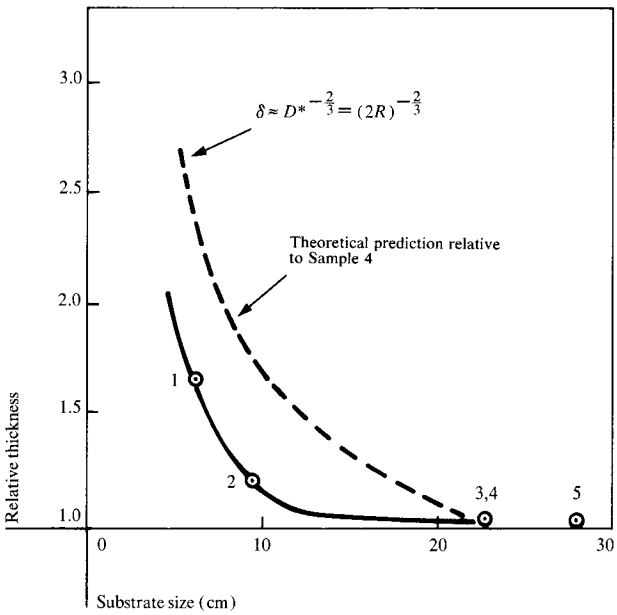

Figure 7 Spin coating thickness relative to Sample 4 as a function of substrate size and shape (see Table 1).

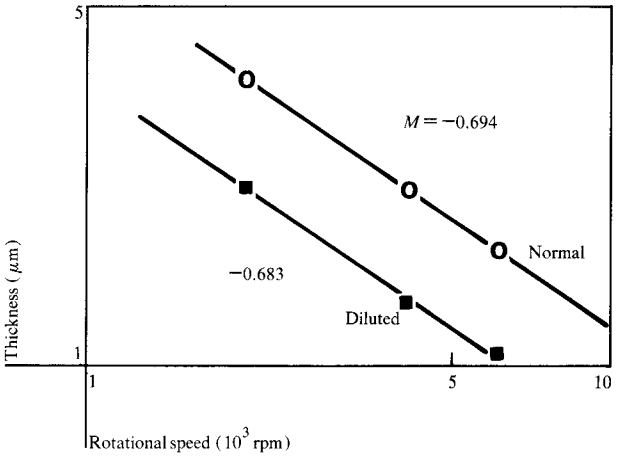

Figure 8 Spin coating thickness of normal (14 percent solids) and diluted (11.5 percent solids) DuPont RC5057; data of Zielinski on silicon wafers [21], $M_{calc} = -0.667$.

Future work should extend the model to treat non-Newtonian solutions (probably most photoresist systems); solutions containing highly volatile solvents; viscoelastic solutions; and transient effects such as constant and variable acceleration (which are known to lead to anomalous results). Further examination of the effects of size and geometry, particularly with non-Newtonian fluids, and the effects of substrate topology, e.g., pattern dimensions and relief surfaces in the case of photoresist systems, is also warranted.

Acknowledgment

The author thanks B. E. Cornish for his valuable assistance with the experiments.

Appendix: Derivation of model equations

The fundamental equation in the derivation of the spin coating model is Eq. (5), namely,

$$\partial\tau_{rz}/\partial z = -\rho r\omega^2, \tag{5}$$

where τ_{rz} is the shear stress on the z face of a fluid element arising from fluid momentum in the r direction. This may be derived by means of two basic approaches: 1) by simplification of either the general equations of fluid motion or the Navier-Stokes equation in cylindrical coordinates, and 2) by a simple, steady state force-balancing on a differential annulus of fluid on the rotating substrate. This Appendix also develops the time-independent and time-dependent solutions, and treats the Coriolis force.

• *Case A: Equations in cylindrical coordinates*

Vector Eq. (1) of the paper can be fully detailed in cylindrical coordinates by reference to any general rheology textbook [22]. For our purposes, consider only the r component of the equation. With reference to Fig. 3,

$$\rho\left[\frac{\partial v_r}{\partial t} + \frac{v_r\partial v_r}{\partial r} + \frac{v_\theta}{r}\left(\frac{\partial v_r}{\partial\theta}\right) - \frac{v_\theta^2}{r} + \frac{v_z\partial v_r}{\partial z}\right]$$

$$= -\frac{\partial p}{\partial r} + \left[\frac{1}{r}\left(\frac{\partial\tau_{rr}}{\partial r}\right) + \frac{1}{r}\left(\frac{\partial\tau_{r\theta}}{\partial\theta}\right) - \frac{\tau_{\theta\theta}}{r} + \frac{\partial\tau_{rz}}{\partial z}\right] + \rho g_r, \tag{A1}$$

where τ_{xx} is the normal stress on the x face of a fluid element and τ_{xy} is the shear stress on the y face of an element arising from momentum in the x direction.

The model invokes the following assumptions to simplify the equations (the θ and z components can be shown to reduce to zero by means of these assumptions):

1. Steady state conditions.
2. Rotationally symmetric flow of a homogenous fluid.
3. No body force or surface force (i.e., complete wetting and initial substrate flooding).
4. Constant pressure flow.
5. Net flow in r direction only.
   a. $v_z \approx 0$,
   b. $v_\theta \approx r\omega$ (angular velocity of rotating disk),
   c. $v_r \ll v_\theta$.
6. Low constant volumetric flow Q in the radial direction (Steady-state assumption $dQ/dt = 0$).

With these assumptions, Eq. (A1) simplifies to

$$\frac{v_r\partial v_r}{\partial r} - \frac{v_\theta^2}{r} = \frac{1}{\rho}\left(\frac{\partial\tau_{rz}}{\partial z}\right). \tag{A2}$$

Then, with the following simplified continuity equation,

$$\frac{1}{r}\left[\frac{\partial(rv_r)}{\partial r}\right] = \frac{\partial v_r}{\partial r} + \frac{v_r}{r} = 0, \tag{A3}$$

and assumptions 5(b) and 5(c), lead to the working phenomenological Eq. (5)

For a Newtonian fluid in this coordinate system, we have

$$\tau_{rz} = \mu\partial v_r/\partial z; \tag{3}$$

and with Eq. (5),

$$\mu\partial^2 v_r/\partial z^2 = -\rho r\omega^2. \tag{6}$$

Equation (6) is the result which one also obtains from the Navier-Stokes equation upon applying assumptions 1 through 5 of the preceding section. In a different but analogous study, Gazley and Charwat [8] and Emslie [11] independently derived a similar equation.

Explicit phenomenological solution

Equation (5) is solved explicitly using the following boundary conditions:

$$\tau_{rz} = \tau_{\max} \qquad \text{for } z = 0,$$

$$\tau_{rz} = 0 \qquad \text{for } z = \delta \tag{A4}$$

(for a free surface).

These lead to

$$\tau_{rz} = \rho t\omega^2(\delta - z) = \tau_{\max}(1 - z/\delta). \tag{A5}$$

The working phenomenological Eq. (A5) can also be derived illustratively by use of a simple model of the process as detailed below.

• *Case B: Steady state force balance on fluid annulus*

Consider Fig. 3 which shows the symmetrical flow pattern of the fluid on the rotating disk. The steady state balance of centrifugal forces shows that

$$\Delta F_c = \Delta m\omega^2 r = 2\pi rz\rho\Delta r\omega^2 r \tag{A6}$$

for a differential annulus. Similarly, the shear force balance is

$$\Delta F_s = \tau_{rz}\Delta A = \tau_{rz}\, 2\pi r\Delta r, \tag{A7}$$

and at steady state,

$$\Delta F_c = \Delta F_s;$$

$$2\pi r\Delta r(z\rho\omega^2 r) = \tau_{rz}\, 2\pi r\Delta r. \tag{A8}$$

One must satisfy the boundary conditions stated in Eq. (A4) and simplification leads to the result

$$\tau_{rz} = \rho\omega^2 r(\delta - z) = \tau_{\max}(1 - z/\delta), \tag{A9}$$

which is equivalent to Eq. (A5).

• *Case C: $dQ/dt = 0$*

By coupling Eq. (A5) or (A9) with Eq. (3), Newton's law of viscosity in one dimension, we compute the velocity gradient as

$$\frac{\partial v_r}{\partial z} = \frac{1}{\mu}(\tau_{rz}) = \frac{\rho r \omega^2}{\mu}(\delta - z). \tag{A10}$$

Equation (A10) is solved by using the following boundary conditions:

$$v_r = 0 \qquad \text{for } z = 0,$$
$$v_r = v_{\max} \qquad \text{for } z = \delta. \tag{A11}$$

Then

$$v_r = v_r(z) = \frac{r\omega^2\delta^2}{\nu}\left[\frac{z}{\delta} - \frac{1}{2}\left(\frac{z^2}{\delta^2}\right)\right]$$
$$= 2v_{\max}\left[\frac{z}{\delta} - \frac{1}{2}\left(\frac{z^2}{\delta^2}\right)\right], \tag{A12}$$

where $\nu = \mu/\rho$.

To determine the velocity profile (Fig. 3) of flow across a thickness of film, we average the velocity over all z:

$$\bar{v}_r = \int_0^\delta 2\pi r v_r(z)dz \Big/ \int_0^\delta 2\pi r dz = \frac{1}{3}\left(\frac{r\omega^2\delta^2}{\nu}\right). \tag{A13}$$

The volumetric flow rate is

$$Q = 2\pi r\delta\bar{v}_r = \frac{2\pi}{3}\left(\frac{r^2\omega^2\delta^3}{\nu}\right), \tag{A14}$$

and the thickness is

$$\delta = \left[\frac{3\pi}{2}\left(\frac{Q\nu}{\omega^2 r^2}\right)\right]^{\frac{1}{3}}. \tag{A15}$$

Averaging over all r, we obtain the average thickness

$$\bar{\delta} = \int_0^R 2\pi r\delta dr \Big/ \int_0^R 2\pi r dr = (81/16\pi)^{\frac{1}{3}}(Q\nu)^{\frac{1}{3}}/(\omega R)^{\frac{2}{3}}. \tag{A16}$$

By converting from the wet to the dry film state,

$$\delta_{\text{dry}} = \delta_{\text{wet}} C_V, \tag{A17}$$

we obtain the final result,

$$\delta = KC_V(\nu/\omega^2 R^2)^{\frac{1}{3}}. \tag{8}$$

• *Case D: $dQ/dt \neq 0$*

The derivation of Eq. (10) follows. Let $\bar{V}$ be the volume of liquid on the disk at any time. Then,

$$d\bar{V}/dt = Q = -\pi R^2\, d\bar{\delta}/dt, \tag{A18}$$

and Eq. (A16) relates Q to the average thickness $\bar{\delta}$, so that

$$\frac{d\bar{\delta}}{dt} = -\frac{16}{81}\left(\frac{\omega^2\bar{\delta}^3}{\nu}\right). \tag{A19}$$

Then, after integrating from $t = 0$,

$$1/\bar{\delta}^2 - 1/\bar{\delta}_0^2 = 0.395\,\omega^2 t/\nu. \tag{A20}$$

When $\bar{\delta} = 0.5\bar{\delta}_0$, the time to achieve half-thickness is

$$t_{0.5} = 7.60\,\nu/\omega^2\bar{\delta}_0^2. \tag{10}$$

The time-dependent equation (9) is derived using a quasi-steady state approach. $\bar{\delta}_0$ is defined as the average thickness at the onset of the region labeled as 3 in Fig. (2), and steady state Eq. (A16) applies.

$$\bar{\delta}_0 = (81/16\pi)^{\frac{1}{3}}(Q_0\nu)^{\frac{1}{3}}/(\omega R)^{\frac{2}{3}}. \tag{A16}$$

Equation (A20) can now be rewritten as

$$\delta/\bar{\delta}_0 = (1 + 0.395\,\omega^2\bar{\delta}_0 t/\nu)^{-\frac{1}{2}}. \tag{A21}$$

Combining Eqs. (A16) and (A21) with Eq. (A17), we eliminate $\bar{\delta}_0$ and obtain for the time-dependent thickness,

$$\delta = \frac{K^{\frac{1}{3}}C_V}{(R\omega)^{\frac{2}{3}}}\left[1 + 0.395\left(\frac{K}{R^{\frac{2}{3}}}\right)^2\left(\frac{\omega^2}{\nu}\right)^{\frac{1}{3}}t\right]^{-\frac{1}{2}}, \tag{A22}$$

where, for substrates with $R > 18$ cm, R is constant, i.e., equal to 18 cm.

• *Case E: Coriolis effect*

The Coriolis force shows its effect as the relative deviation of the angular velocity v_θ from the local disk velocity ωR, or $(\omega R - v_\theta)/\omega R$. This deviation factor, if it is significant, affects assumption 5(b) of Case A (where $r = R$) of the model; the effect can be calculated as follows.

The Coriolis force perpendicular to the radius (and opposite in direction to ω) for the differential annulus of Case B is

$$\Delta F = \Delta m 2 v_r \omega. \tag{A23}$$

A steady state force balance for the *net* circumferential flow, $(R\omega - v_\theta)$, is similar to that of Case B:

$\Delta F_{\text{shear}} = \Delta F_{\text{coriolis}}$, or

$$2\pi R\Delta R\mu\left(\frac{dv_\theta^1}{dz}\right) = 2\pi R\Delta R\rho\delta\left(1 - \frac{z}{\delta}\right)^2 v_r\omega, \tag{A24}$$

where $v_\theta^1 = R\omega - v_\theta$ is the net flow in the θ direction. On simplifying we have

$$dv_\theta^1/dz = \frac{2v_r\omega\delta}{\nu}\left(1 - \frac{z}{\delta}\right). \tag{A25}$$

Then, integrating over z, we obtain

$$v_\theta^1 = \frac{2v_r\omega\delta}{\nu}\left(\frac{z}{\delta} - \tfrac{1}{2}\frac{z^2}{\delta^2}\right) \text{ and} \tag{A26}$$

$$v_{\theta\max}^1 = \rho v_{r\max}\omega\delta^2/\nu. \tag{A27}$$

Using (A12) we have

$$v_{r\max} = \omega^2 R\delta^2/2\nu. \tag{A28}$$

If we combine Eqs. (A28) and (A29),

$$v_{\theta\max}^1 = (\omega R)/2\,(\omega\delta^2/\nu)^2; \tag{A29}$$

but

$$v_{\theta\max}^1 = \omega R - v_\theta, \tag{A30}$$

so that

$$(\omega R - v_\theta)/\omega R = \tfrac{1}{2}\left(\frac{\omega\delta^2}{\nu}\right)^2. \quad \text{(A31)}$$

For $\omega/2\pi = 2000$ rpm, $\delta = 1$ μm and $\nu = 0.125$ cm^2/s thus,

$$(\omega R - v_\theta)/\omega R = 1.4 \times 10^{-10}. \quad \text{(A32)}$$

A similar value may be obtained using the analytical results for the velocity deviation factor of Gazley and Charwat [8] under these conditions.

References

1. L. R. Martinson, "Microresist Technology," in *Proceedings of the Kodak Seminar on Microminiaturization*, Kodak Park, Rochester, New York, June 1965.
2. G. C. Schwartz, "Thickness Studies on Exposed Kodak Thin Film Resist Films," in *Proceedings of the Kodak Seminar on Microminiaturization*, Kodak Park, Rochester, New York, June 1965.
3. C. J. Taylor, "Superior Photograving Process for Semi-Conductor Devices," *NASA CR-597*, U.S. Government Publication G-2003, September 1966.
4. *Kodak Photosensitive Resists for Industry*, Kodak Industrial Handbook, Kodak Park, Rochester, New York, 1962.
5. G. D. Fulford, "The Flow of Liquids in Thin Films," in *Advances in Chemical Engineering*, Vol. 5, Academic Press, Inc., New York, 1964, p. 151.
6. H. Epsig, "Heat Transfer by Condensation of Steam on a Rotating Disc," Ph.D. Thesis, University of London, England, 1964.
7. L. A. Dorfman, "Heat Transfer and Viscous Liquid Flow on a Rotating Disk," *J. Eng. Phys.* **12,** 309 (1967).
8. C. Gazley, Jr. and A. F. Charwat, "The Characteristics of a Thin Liquid Film on a Spinning Disk," *No. AD669557*, The Rand Corporation, Santa Monica, California, May 1968, p. 3851.
9. P. H. Walker and J. G. Thompson, *Proc. Am. Soc. Testing Materials (Part 2)* **22,** 464 (1922).
10. L. R. Kleinschmidt, *Bull. Am. Soc. Testing Materials, No. 193*, p. 53 (1953).
11. A. G. Emslie, F. T. Bonner, and C. G. Peck, "Flow of a Viscous Liquid on a Rotating Disk," *J. Appl. Phys.* **29,** 858 (1958).
12. A. Acrivos, M. J. Shah, and E. E. Petersen, "On the Flow of a Non-Newtonian Liquid on a Rotating Disk," *J. Appl. Phys.* **11,** 963 (1966).
13. H. Epsig and R. Hoyle, "Waves in a Thin Layer on a Rotating Disk," *J. Fluid Mech. (Part 4)* **22,** 671 (1965).
14. W. Nusselt, *Zeitschrift des Vereins Deutscher Ingenieur* **60,** 541 (1916).
15. H. Grimley, "Liquid Flow Conditions in Packed Towers," *Inst. Chem. Eng. Trans.* **23,** 228 (1945).
16. P. L. Kapitsa, "Wave Formation of a Thin Layer of a Viscous Liquid," *Sov. Phys.—JETP* **18,** 3 (1948).
17. A. M. Binnie, "Experiments on Onset of Wave Formation on Films of Water Flowing Down a Vertical Plane," *J. Fluid Mech.* **2,** 551 (1957).
18. B. T. Benjamin, "Wave Formation in Laminar Flow Down an Inclined Plane," *J. Fluid Mech.* **2,** 554 (1957).
19. J. Aroesty, J. F. Gross, M. M. Illickal, and J. V. Maloney, "Blood Oxygenation: A Study in Bioengineering Mass Transfer," The Rand Corporation, Santa Monica, California, November 1967, p. 3732.
20. R. Kelley, "Relationships Between Resist Thickness and Pinholing," in *Proceedings of the Kodak Seminar on Microminiaturization*, Kodak Park, Rochester, New York, June 1965.
21. L. Zielinski, private communication, IBM System Products Division, E. Fishkill, New York, January 1975.
22. J. M. McKelvey, *Polymer Processing*, John Wiley & Sons, Inc., New York, 1962.

Received April 1976; revised November 1976

The author is located at the System Products Division development laboratory, Boardman Road, Poughkeepsie, New York 12602.